35th Annual International Conference of the IEEE EMBS
Osaka, Japan, 3 - 7 July, 2013

Comparison of Neuronal Excitation between Extruded Slab Partial Head Model and Full Head Model in Subdural Cortical Stimulation

Hyeon Seo, Donghyeon Kim, Sung Chan Jun*

Abstract— **Cortical stimulation (CS) is an appealing and emerging treatment for neurological disorders. CS is known to promote functional recovery effectively; however, its underlying mechanism and the optimal parameters for the effective treatment are not clearly understood. In this work, we developed a realistic three-dimensional full head and chest model for subdural CS. Our proposed model was compared at the neuron level with an existing simplified extruded slab partial head model depicting around precentral gyral cortex only. Each model was coupled with the pyramidal neuronal model in order to investigate an extent of neuronal excitation. We found that the crown of the cortex was the most excitable area in the unipolar stimulation, while in the bipolar stimulation, the lip and bank were excited more easily than other areas. Finally, it was evident that our proposed model was substantially different in excitation threshold from the existing simplified model, which is compelling to do computational CS study on more realistic head models.**

I. Introduction

Cortical stimulation (CS) is one of the electrotherapies used to deliver electrical power to the brain for expediting neuronal modulation or stimulation, and it has been used increasingly as a treatment for chronic pain, stroke rehabilitation, epilepsy, and other brain disorders [1-4]. These CS approaches via either invasive (surgical implantation of electrodes) or noninvasive (transcranial magnetic (TMS) or electrical stimulation (tDCS)) methods have advantages over other extensive therapies. Especially, invasive CSs show enhanced therapeutic effects on chronic pain and movement disorders compared to noninvasive CSs [1, 2]. Among invasive methods, there are epidural cortical stimulation (ECS, in which electrodes are located directly on the dura mater) and subdural cortical stimulation (SuCS; electrodes are placed on the cerebral surface and beneath the dura mater). While ECS is less risky and is used more generally than SuCS, SuCS is useful for some patients who suffer from advanced cortical atrophy due to duro-cortical separation. In addition, SuCS may convey more acute focal electrical stimulation to the exposed cortex, thus decreasing the loss of current.

Recent studies that seek optimal stimulation parameters and an in-depth understanding of underlying mechanisms of CS have been conducted through computational approaches with head/brain models [5-8]. These authors developed the computational extruded slab partial head model, which is a simplified model depicting the precentral gyrus area only of the brain. In addition, realistic full head models based on human MRI were proposed in tDCS [9] and in CS [10]. They used these computational models to analyze the effects of CS and estimated the current density distributions and activating functions. However, these results are insufficient to understand the precise polarization of neurons and stimulation thresholds in the neuron level. In order to investigate neuronal activation in more detail, some researchers developed compartmental neuronal models, which were then coupled to computational existing head models [11-13]. However, these studies focused on ECS, but not SuCS. Further, they used the extruded slab partial head model, which is so crude that it may produce a less accurate prediction of neuronal activation due to geometric model mismatch.

In this work, we investigated the mechanism of SuCS. For this purpose, a realistic three-dimensional full head and chest model was developed to estimate the distribution of current density in the brain for various input voltages. In addition, the compartmental neuronal model was coupled to this model, and finally neural activation was estimated up to the neuron level. We modeled layer 5 pyramidal neurons located along the cortex. Both the extruded slab model and the realistic head model were considered and two different polarities (unipolar and bipolar) were compared as well.

II. Methods

A. The 3D computational models

We developed two kinds of three-dimensional computational models for SuCS. One is an extruded slab partial head model that represents the precentral gyrus and its surrounding sulci and gyri. This is the most simplified brain model which has been used widely for computational studies of CS. This model consists of white matter, gray matter, cerebrospinal fluid (CSF), dura mater, and skull. The conductivities for each layer are tabulated in Table 1, which was obtained from the literatures [5, 8, 10, 11, 14]. Particularly, the white matter conductivity was considered to be anisotropic, yielding a higher value perpendicular to the skull. For more details of this model, refer to [7].

The other is a realistic full head and upper body model. From whole head and body MRI data [15], realistic head and body shapes were extracted. Particularly, white matter, gray matter, CSF, ventricle, cerebellum, skull, and scalp were segmented reasonably to generate this model. The same conductivities of each layer as those in the extruded slab model were assigned. For SuCS, disk type electrodes were attached on the gray matter (beneath the dura mater) and were designed to be covered with substrate. For comparison with the extruded slab model, two electrodes were place on the

This work was supported by the National Research Foundation (NRF) funded by the Korean Government (NRF-2010-0026438).

H. Seo, D. Kim and S.C. Jun are with the School of Information and Communications, Gwangju Institute of Science and Technology, Gwangju, South Korea (*Corresponding author: scjun@gist.ac.kr).

precentral gyrus. The detailed model is illustrated in Fig. 1 and 2.

These computational models were analyzed in COMSOL Multiphysics (version 4.2a; Burlington, MA) and computed by the finite element method. For the extruded slab model, about 250,000 tetrahedral elements were used. For the realistic head model, about 4.3 million tetrahedral elements were used. The bi-conjugate gradient method with preconditioning incomplete Cholesky factorization was applied to solve these computational models.

TABLE I. CONDUCTIVITIES OF TISSUES AND ELECTRODES [8,10,14]

Compartment	*Conductivity (S/m)*
Substrate conductivity	0.1×10^{-9}
Electrode conductivity	9.4×10^{6}
Scalp	0.465
Skull	0.01
Dura mater	0.065
CSF	1.65
Gray matter	0.276
White matter (parallel to fibers)	1.1
White matter (perpendicular to fibers)	0.13

B. The pyramidal neuronal models

For simplicity, only the layer 5 (L5) pyramidal neurons were modeled here. The detailed morphology and electrical properties of cortical neurons from cat visual cortex [16] were used for neuron modeling, and were modified to fit human brain geometry [11]. These neuronal models were implemented by NEURON [17]. Due to its complexity and the limitation of computational resources, such neurons could not be constructed directly in the three-dimensional head/brain models. Thus, we computed extracellular electric potentials distributed within the brain (induced by current/voltage input) through the computational head/brain models addressed in the previous section. These extracellular electric potentials were considered as input potentials to excite or evoke neurons. That is, they were assumed to be applied by extracellular stimulation in 100 μs monophasic pulses. Through these processes, we investigated the neuronal responses in various locations thoroughly. We declared a neuron to be excited when the membrane potential of one node in the corresponding neuron model was raised by 70 mV or more above the resting potential [13].

We considered neurons to be located under the disk electrode in the three-dimensional models. As shown in Fig. 3, seven types of neurons were modeled, and each was considered to be represented in the designated region. These neurons were located in the cross section perpendicular to the electrodes. In the realistic head model especially, slight manual adjustments were made to the neurons because the thickness of the gray matter and the depth of sulci are not uniform over the cortex, as shown in Fig. 4. The soma and dendrites of L5 pyramidal neurons were located within the gray matter, and the axons penetrated to the white matter. Thus, the soma was located 0.5 mm above the boundary

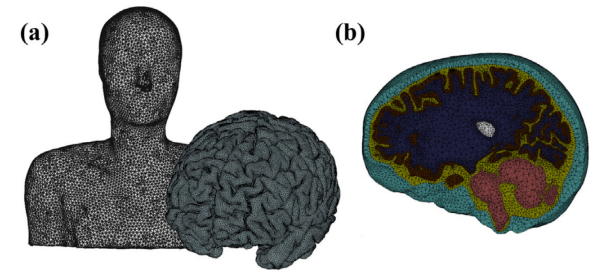

Figure 1. (a) Mesh of realistic full head and upper body model; (b) cross section of realistic brain model, upper body excluded

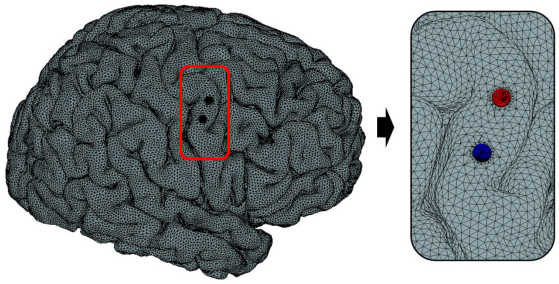

Figure 2. Electrode arrangement in realistic head model; two disk type electrodes attached on precentral gyrus

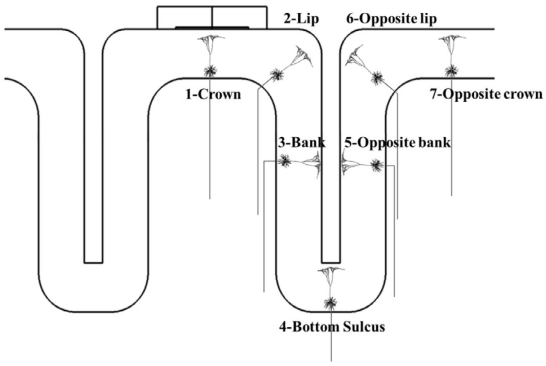

Figure 3. Neuronal model distribution in extruded slab model; they are distributed in the cross section and each neuron represents the region of the crown, lip, bank, bottom sulcus, opposite bank, opposite lip, and opposite crown. Each neuronal model is numberd from left to right

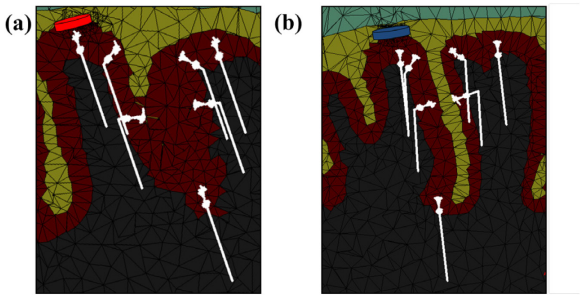

Figure 4. Neuronal model distribution in realistic brain model; (a) the cross sections perpendicular to the top electrode and (b) bottom electrode shown in Figure 2

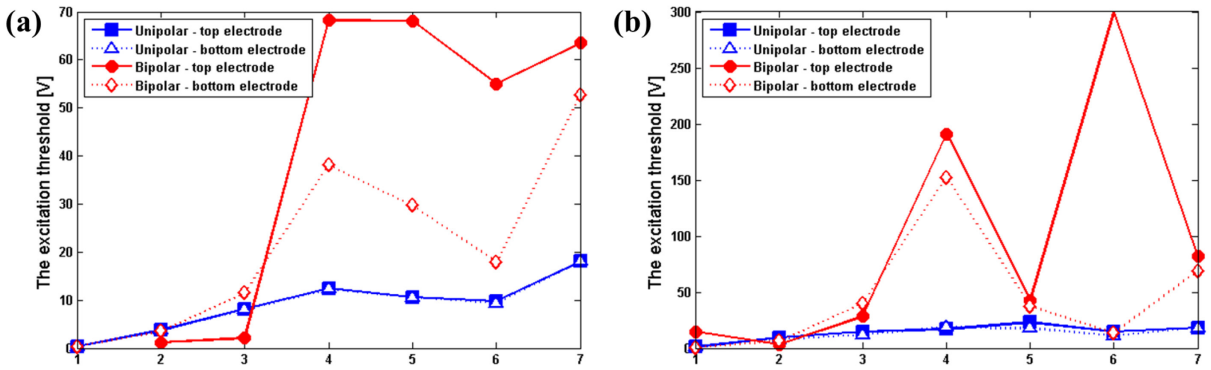

Figure 5. The excitation thresholds of individual neurons in (a) extruded slab model and (b) realistic brain model; x-axis indicates the number of neurons, such that 1 indicates the neurons in the crown and 7 indicates the neurons in the opposite crown

between the white and gray matters [13]. All neurons were oriented perpendicular to the gray matter surface.

C. *Polarity of Stimulation*

For bipolar or unipolar stimulations, we observed neuronal activation over varying stimulus inputs. For simplicity, in the bipolar stimulation the top electrode (red in Fig. 2) was considered a cathode and the bottom electrode an anode. In the unipolar stimulation, both electrodes were anode. For each neuron, we estimated the excitation threshold as the smallest input voltage that excited neurons at a given location.

III. Results

A. *Bipolar versus unipolar stimulations*

First, we explored the excitation thresholds in the extruded slab model, as shown in Fig. 5(a). In the unipolar stimulation, neurons under both electrodes showed the same excitation thresholds. The threshold in the unipolar stimulation was lowest in the crown, and increased as it moved from the lip to the bottom of the sulcus, farther from the electrode. Further, the opposite crown had a higher threshold than the opposite lip and bank. In the bipolar stimulation, the top electrode was considered cathode and the bottom electrode anode. Here, the neurons under the anode yielded comparable thresholds to those in the unipolar stimulation of the crown and lip, while they yielded higher thresholds in other regions due to the effect of the cathode. Although in both bipolar and unipolar stimulations, the crown was the most excitable by anodic stimulation, cathodic stimulation did not excite the neurons in the crown. However, neurons in the bank and lip had lower thresholds with cathodic than anodic stimulation.

Second, we investigated excitation thresholds in the realistic full head and upper body model. As shown in Fig. 5(b), thresholds to unipolar stimulation between both electrodes were quite similar despite the different brain geometry. The crown and opposite crown in particular had the same thresholds. However, neurons under the top electrode had higher thresholds than for the bottom electrode, except in the bottom sulcus. In bipolar stimulation, the lip was the most excitable area, followed by the crown. The lip and bank were more readily excited by cathodic than anodic stimulation. In addition, the opposite lip under the cathode seemed to have higher thresholds than other regions.

B. *The effect of head/brain model geometry*

We simulated bipolar and unipolar SuCSs using the extruded slab model and the realistic head/chest model. In unipolar stimulation, excitation increased when neurons were farther away from electrodes. However, thresholds in the realistic head and chest model were substantially higher than those in the extruded slab model, and the differences became noticeably larger in the bottom sulcus and opposite bank. In bipolar stimulation, the lip and bank were excitable by cathode and the crown and lip were activated by anode under 10V stimulus input in both models. We found that the overall thresholds were higher in the realistic brain model than the extruded slab model, particularly far higher in the bottom sulcus and opposite lip.

IV. Discussion

In this paper, we investigated bipolar and unipolar SuCSs to estimate the activation of pyramidal neurons over varying input voltages. To understand the effect of model mismatch, we considered not only the extruded slab model, but also the realistic head/chest model; the latter yielded a relatively far smaller model mismatch. In order to investigate neuronal activation at the neuron level, these computational models were coupled with the pyramidal neuronal models. We observed that excitation thresholds varied according to electrode polarity and model geometry.

A. *Comparison with previous modeling studies*

As in Manola's study [8, 12], we found that cathodic stimulation could not activate neurons located directly beneath the cathode in the extruded slab model. In contrast to this result, other studies reported activation by cathodic stimulations when axon collaterals were included in the

pyramidal neuronal model [13, 18]. It was reported in [13] that action potentials could propagate from collaterals to the main axons according to differences in diameter between them. However, we observed the excitation of neurons oriented perpendicular to the cathode in the realistic brain model. We found that, without the inclusion of collateral axons, the model geometry also affected neuron activation. Further, we found that cathodic, rather than anodic, stimulation could excite deeper regions of the bank at relatively lower thresholds. Therefore, cathodic stimulation appears to favor the excitation of neurons parallel to the electrode surface. This is in agreement with other modeling studies [8, 11, 12].

B. The effect of head/brain geometry

In this paper, we used two kinds of head/brain models. A realistic head model was generated based on human MRIs, so it had some variation in gray matter thickness and sulci depths. In contrast, in the extruded slab model, the thickness of the gray matter and depths of sulci were uniform. For example, in the extruded slab model, the distance between the electrode and bottom sulcus was 17.27 mm, while in the realistic brain model, it was 24.17 mm and 24.85 mm for top and bottom electrodes, respectively. Thus, neurons in the realistic head model seemed slightly farther from the electrodes than those in the extruded slab model; this may have affected the excitation thresholds. We found that the overall excitation thresholds in the realistic brain model were notably higher than those in the extruded slab model, with differences far higher in the bottom of the sulci.

C. The limitation of this work

We developed the realistic head and chest model from MRI data. Especially, we focused on generating head model as accurately as we can. However, due to intractable computation load, chest model was produced to yield the realistic shape and was considered uniform conductor, to which conductivity value of the scalp was assigned. We found that the inclusion of chest model affected our analysis. Considering the whole body is not that substantially different, we expect. Input electrodes and reference electrode are far away from the remaining body; thus their role may be negligibly small.

In this work, we investigated to focus on the precentral gyrus motor cortex for the comparison between two computational models. In-depth study on other cortex or the whole brain should be more beneficial and impacted, which is under study.

REFERENCES

[1] S. Canavero, *Textbook of Therapeutic Cortical Stimulation*. 2009.

[2] E. B. Plow, J. R. Carey, R. J. Nudo, and A. Pascual-Leone, "Invasive cortical stimulation to promote recovery of function after stroke: A critical appraisal," *Stroke*, vol. 40, no. 5, pp. 1926–1931, May 2009.

[3] J. A. Kleim, R. Bruneau, P. VandenBerg, E. MacDonald, R. Mulrooney, and D. Pocock, "Motor cortex stimulation enhances motor recovery and reduces peri-infarct dysfunction following ischemic insult," *Neurological Research*, vol. 25, no. 8, pp. 789–793, Dec 2003.

[4] H. I. Kim, Y. I. Shin, S. K. Moon, G. H. Chung, M. C. Lee, and H. G. Kim, "Unipolar and continuous cortical stimulation to enhance motor and language deficit in patients with chronic stroke: Report of 2 cases," *Surgical Neurology*, vol. 69, no. 1, pp. 77–80, Jan 2008.

[5] A. Wongsarnpigoon and W. M. Grill, "Computational modeling of epidural cortical stimulation," *Journal of Neural Engineering*, vol. 5, no. 4, pp. 443–454, Dec 2008.

[6] D. Kim, S. C. Jun, and H. I. Kim, "Computational study of subdural and epidural cortical stimulation of the motor cortex," In *proc. 33th Int. Conf. IEEE Engineering in Medicine and Biology Society*, pp. 7226–7229, 2011.

[7] H. Seo, D. Kim, and S. C. Jun, "A comparative study of the 3D precentral gyrus model for unipolar and bipolar current stimulations," In *proc. 34th Int. Conf. IEEE Engineering in Medicine and Biology Society*, pp. 1892–1895, 2012.

[8] L. Manola, B. H. Roelofsen, J. Holsheimer, E. Marani, and J. Geelen, "Modelling motor cortex stimulation for chronic pain control: Electrical potential field, activating functions and responses of simple nerve fibre models," *Medical and Biological Engineering and Computing*, vol. 43, no. 3, pp. 335–343, May 2005.

[9] A. Datta, V. Bansal, J. Diaz, J. Patel, D. Reato, and M. Bikson, "Gyri-precise head model of transcranial DC stimulation: Improved spatial focality using a ring electrode versus conventional rectangualr pad," *Brain Stimulation*, vol. 2, no. 4, pp. 201–207, Oct 2009.

[10] D. Kim, H. Seo, H. Kim, and S. Jun, "The computational study of subdural cortical stimulation: A quantitative analysis of voltage and current stimulation," In *proc. 34th Int. Conf. IEEE Engineering in Medicine and Biology Society*, pp. 867–870, 2012.

[11] A. Wongsarnpigoon and W. M. Grill, "Computer-based model of epidural motor cortex stimulation: Effects of electrode position and geometry on activation of cortical neurons," *Clinical Neurophysiology*, vol. 123, no. 1, pp. 160–172, Jan 2012.

[12] L. Manola, J. Holsheimer, P. Veltink, and J. R. Buitenweg, "Anodal vs. cathodal stimulation of motor cortex: A modeling study," *Clinical Neurophysiology*, vol. 118, no. 2, pp. 464–474, Feb 2007.

[13] D. G. Zwartjes, T. Heida, H. K. Feirabend, M. L. Janssen, V. Visser-Vandewalle, H. C. Martens, and P. H. Veltink, "Motor cortex stimulation for Parkinson's disease: A modeling study," *Journal of Neural Engineering*, vol. 9, no. 5, pp. 056005, Oct 2012.

[14] P. W. Nicholson, "Specific impedance of cerebral white matter," *Experimental Neurology*, vol. 13, no. 4, pp. 386–401, Dec 1965.

[15] M. Windhoff, A. Opitz, and A. Thielscher, "Electric field calculations in brain stimulation based on finite elements: An optimized processing pipeline for the generation and usage of accurate individual head models," *Human Brain Mapping*, Nov 2011, doi: 10.1002/hbm.21479.

[16] Z. F. Mainen and T. J. Sejnowski, "Influence of dendritic structure on firing pattern in model neocortical neurons," *Nature*, vol. 382, no. 6589, pp. 363–366, Jul 1996.

[17] M. L. Hines and N. T. Carnevale, "The NEURON simulation environment," *Neural Computation*, vol. 9, no. 6, pp. 1179–1209, Aug 1997.

[18] R. Salvador, S. Silva, P. J. Basser, and P. C. Miranda, "Determining which mechanisms lead to activation in the motor cortex: A modeling study of transcranial magnetic stimulation using realistic stimulus waveforms and sulcal geometry," *Clinical Neurophysiology*, vol.122, no. 4, pp. 748–758, Apr 2011.